A Direct Real-Time Spectroscopic Investigation of the Mechanism of Open Complex Formation by T7 RNA Polymerase†

Srinivas S. Sastry* and Barbara M. Ross

Laboratory of Molecular Genetics, Box 174, The Rockefeller University, New York, New York 10021

Received March 26, 1996; Revised Manuscript Received October 10, 1996⊗

ABSTRACT: Initiation of transcription occurs through a series of steps starting with the binding of RNA polymerase to a promoter DNA and formation of a closed complex. The closed complexes, then isomerize to open complexes. In the open complexes a portion of the promoter DNA is unwound. Using fluorescence spectroscopy, we have investigated in real-time the mechanism of unwinding of promoter DNA during the transition from closed to open complexes of T7 RNA polymerase. We synthesized DNA templates containing the fluorescent base analog 2-aminopurine in place of adenine at specific positions in a T7 RNA polymerase promoter. We located the 2-aminopurine residues in the presumed melting domain of the promoter at −1, −4, and at −6. The fluorescence of 2-aminopurine increases when the DNA goes from a double-stranded form to a single-stranded form. By spectroscopically monitoring the increase in fluorescence of 2-aminopurine in DNA−T7 RNA polymerase complexes, we obtained kinetic and thermodynamic information for DNA unwinding. In the presence of the initiating nucleotide GTP, conformational transitions in the polymerase−promoter complex leading to strand opening were slower than in its absence. The rate of base pair disruption at −1, −6, and at −4 was also slower in the presence of GTP than in its absence. At 37 °C, base pair disruption occurred first at −1 followed by −6 and finally at −4. Open complex formation was temperature-sensitive. Temperature effects at −1, −6, and at −4 were consistent with this order of base pair disruption. The apparent activation energies (E_a) for base pair disruption around −1 and −6 were 14 kcal mol^{-1} and 50 kcal mol^{-1}, respectively, also suggesting this order of base pair disruption. Transcription initiation assays using G-ladder synthesis revealed that initiation rates were almost the same on all three templates containing the modified base. Unlike strand opening, we did not observe lag times for G-ladder synthesis. We suggest that facile base pair disruption at −1 is sufficient for transcription initiation. Based on these data, it is proposed that the polymerase makes contacts at or near −1 and −6 resulting in untwisting of these base pairs thus creating at least two base pair disruption events at −1 and at −6, which are followed by bidirectional propagation to −4.

Initiation of procaryotic transcription involves a complex set of transitions beginning with the binding of RNA polymerase (R) to promoter DNA (P) (McClure, 1985). Equation 1 describes the overall mechanism of initiation of transcription. The recognition of the promoter leads to formation of closed complexes (RP_c):

$$R + P \underset{k_{-1}}{\overset{k_1}{\rightleftharpoons}} RP_c \underset{k_{-2}}{\overset{k_2}{\rightleftharpoons}} RP_o \xrightarrow{NTPs} RNA \qquad (1)$$

where k is a rate constant for the reaction step.

In the closed complexes, the promoter DNA is in double-stranded form. The closed complexes, isomerize to open complexes, in which the DNA is partially melted (RP_o) [for a review, see deHaseth and Helmann (1995)]. In the presence of NTPs, RP_o begins synthesis of RNA. There are intermediates between RP_c and RP_o, and probably several types of complexes at each step depending on the promoter sequence, the temperature, and the ionic strength [for example, see Buc and McClure (1985), Cowing et al. (1989), Kovacic (1987), Krummel and Chamberlin (1989), Mecsas et al. (1991), Roe, et al. (1985), Sen and Dasgupta (1995), Spassky et al. (1985) and Suh et al. (1992a,b)]. While in the case of *Escherichia coli* RNAP it has been estimated that ∼17 base pairs (bp)[1] of promoter DNA are disrupted in open complexes (Amouyal & Buc, 1987; deHaseth & Helmann, 1995; Gamper & Hearst, 1982), corresponding estimates for T7 RNAP have been less reliable. Although it has been implicitly accepted that the overall initiation reaction for T7 RNAP follows eq 1, so far RP_c and RP_o have not been experimentally separated nor have any intermediates been identified. Further complexities in the mechanism of T7 RNAP initiation were apparent from the fact that segments of the nontemplate strand in the promoter can be deleted without seemingly affecting the rates or the correctness of initiation (Maslak & Martin, 1993).

We have investigated the mechanism of open complex formation using the fluorescence of 2-aminopurine as a probe. 2-AP is an analog of adenine that can form a Watson−Crick type of base pair with thymine in double-

† S.S.S. is a Louis B. Mayer Foundation Fellow, and is grateful for a financial grant from the Mayer Foundation. We thank the Hewlett-Packard Co. for awarding an HPLC instrumentation grant and service contracts.

* Corresponding author. Telephone: 212-327-8987. FAX: 212-327-8651. E-Mail: sastrys@rockvax.rockefeller.edu.

⊗ Abstract published in *Advance ACS Abstracts,* December 1, 1996.

[1] Abbreviations: 2-AP, 2-aminopurine; T7 RNAP, bacteriophage T7 RNA polymerase; TBE, 180 mM Tris−borate−2 mM EDTA buffer; HPLC, high-performance liquid chromatography; ss, single-stranded; ds, double-stranded; bp, base pair(s); PC, personal computer; UM, unmodified template.

S0006-2960(96)00729-5 CCC: $12.00

stranded DNA (Figure 1A). The global structure of the DNA remains in B-form, and the substituted DNA is recognized by DNA-binding proteins (McLaughlin et al., 1987; Nordlund et al., 1989; Xu et al., 1994). In contrast to normal DNA bases, 2-AP exhibits strong fluorescence when excited at wavelengths above (>300 nm) the UV absorption range of normal DNA bases (<260−280 nm). The fluorescence of 2-AP is sensitive to its microenvironment (Ward et al., 1969). Previous work has demonstrated that 2-AP is an excellent probe for monitoring local changes in DNA and in DNA−protein complexes [e.g., see Bloom et al. (1993), Frey et al. 1995), Hochstrasser et al. (1994), Nordlund et al. (1989, 1993), Raney et al. (1994) and Xu et al. (1994)].

In this work, we constructed templates with 2-AP at three different sites in a T7 RNAP promoter, and formed promoter complexes with T7 RNAP. We observed promoter melting by T7 RNAP as a steady-state increase in fluorescence of 2-AP. Analysis of promoter melting under different conditions revealed new information regarding the mechanism of T7 RNAP open complex formation.

MATERIALS AND METHODS

DNAs and Proteins. DNA oligonucleotides with and without 2-AP were commercially synthesized by automated solid phase procedures (Midland Reagent Co., Midland, TX) and further purified by HPLC. The concentrations of DNAs were calculated from their respective molar extinction coefficients at 260 nm ($\sim 10^4$ M^{-1} cm^{-1} per nt). Because of the low extinction coefficient of 2-AP at 260 nm (10^3 M^{-1} cm^{-1}), its contribution to the cumulative absorbance of the DNA bases is negligible (Fox et al., 1958). Stock solutions of ds oligonucleotides (10 μM) were prepared by mixing equimolar amounts of 2-AP strand with unmodified complementary oligo in 50 mM Tris-HCl, pH 7.5, + 7 mM $MgCl_2$ (Tris−Mg^{2+} buffer). The oligos were heated to 65 °C and cooled slowly overnight. Polynucleotide kinase was purchased from New England Biolabs (Beverly, MA). rNTPs were purchased from Pharmacia Biotech. Inc. (Piscataway, NJ) at a concentration of 100 mM. T7 RNAP was prepared locally according to the procedure of Goldberg and Dunn (1988) and also by a procedure that was modified by Zawadzki and Gross (1991). The concentration of the purified enzyme was determined using a molar extinction coefficient of $\epsilon_{280} = (1.4 \pm 0.1) \times 10^5$ (Goldberg & Dunn, 1988).

DNA-Binding Assay. 23/27-mers (0.5 pmol) were labeled at their 5′ ends with ^{32}P and added to Tris−Mg^{2+} buffer kept on ice. T7 RNAP was added at various concentrations to each binding reaction separately. The final volume of the reaction was 50 μL. The binding reaction was transferred to 37 °C for 10 min, and then glycerol was added to 5% final concentration. Loading dyes were not added. The reactions were run on an 8% acrylamide−TBE nondenaturing gel (14 cm × 16 cm). Before the samples were deposited in the gel, it was pre-run and the tank buffer was replaced with fresh buffer. The samples were electrophoresed at 5 V/cm until the bromophenol blue dye (added in separate lanes from sample lanes) was 2−3 cm from the bottom of the gel. The gels were soaked for 20 min in 5% acetic acid + 5% MeOH + 3% glycerol, dried, and autoradiographed. Binding data were obtained by first calculating the fractional binding as follows: $[BL_b/(BL_b + BL_f)] - [C/(C + C_f)]$ where BL_b is the integrated band area from the storage phosphor signal representing the bound DNA, BL_f is the band area representing the free DNA in the same lane, C is the band area in the control (no T7 RNAP), and C_f is the band area corresponding to the free DNA in the same lane. All band areas were obtained by first subtracting nonspecific background phosphor counts from a portion of the gel where no bands were present. All quantitations were done with the aid of the ImageQuant program using a phosphorimager.

Transcription Assay. For G-ladder synthesis, 0.2 μM 23/27 bp template was mixed with 50 μM GTP containing 15 pmol of [α-^{32}P]GTP (specific radioactivity 3000 Ci/mmol; New England Nuclear) in Tris−Mg^{2+} buffer (see above). T7 RNAP was then added to 0.2 μM, and the reaction mixture (50 μL) was incubated at various temperatures. Two and a half microliter aliquots of the reaction were withdrawn at different time points, mixed with 5 μL of 8 M urea−TB−10 mM EDTA, heated in a boiling water bath for 5 min, and run on a 24% acrylamide−TBE−8 M urea gel. The transcripts were visualized by autoradiography, and the percent ^{32}P incorporation was measured directly by counting the ^{32}P in gel strips containing the G-ladder.

Steady-State Fluorescence Measurements. Template oligos were diluted to 0.1 μM in Tris−Mg^{2+} buffer. The DNA sample (500 μL) was loaded in a thermostated quartz cuvette that was stirred in a Hitachi F-2000 spectrofluorometer. The sample was equilibrated at specified temperatures for at least 5 min before measurements were commenced. The excitation and emission wavelengths were set at 310 nm and 360 nm, respectively, with a band width of 5 nm. T7 RNAP (in 25 μL; 0.1 μM final concentration) was added to the oligo solution, and the fluorescence data were acquired using a PC that was interfaced to the spectrofluorometer. The data were signal-averaged and digitized at 2 s intervals by the instrument. Addition of T7 RNAP caused a ∼30% base-line jump in steady-state fluorescence of the sample. This value was subtracted from the kinetic data. Addition of T7 RNAP to buffer only also caused a ∼30% immediate jump. Addition of an equal volume of T7 RNAP storage buffer to oligonucleotide templates did not cause the fluorescence jump. The increase in base-line fluorescence intensity when T7 RNAP was added to ds oligo solution is probably because of the unusually large number of Trp in T7 RNAP (19; 2.15 mol %). Here, the base-line fluorescence of ds oligos is smaller compared to ss oligos. This base-line value was corrected by subtracting the contribution from T7 RNAP in our data. The fluorescence intensity of a 0.1 μM solution of T7 RNAP remained constant for several hours. This indicated that any change in the steady-state fluorescence of mixtures of T7 RNAP plus 2-AP ds DNAs was only due to changes in the microenvironment of 2-AP. Because there was no overlap between the absorption spectrum of T7 RNAP and the emission spectrum of 2-AP (see Figure 2), Forster energy transfer considerations do not apply here. Inner-filter effects were not considered because the absorbance of 2-AP at the excitation wavelength was very small (<0.02) and was nonexistent at the emission wavelength.

RESULTS

Rationale. The fluorescence intensity of 2-AP increases ∼2−3-fold when the complementary DNA strands separate

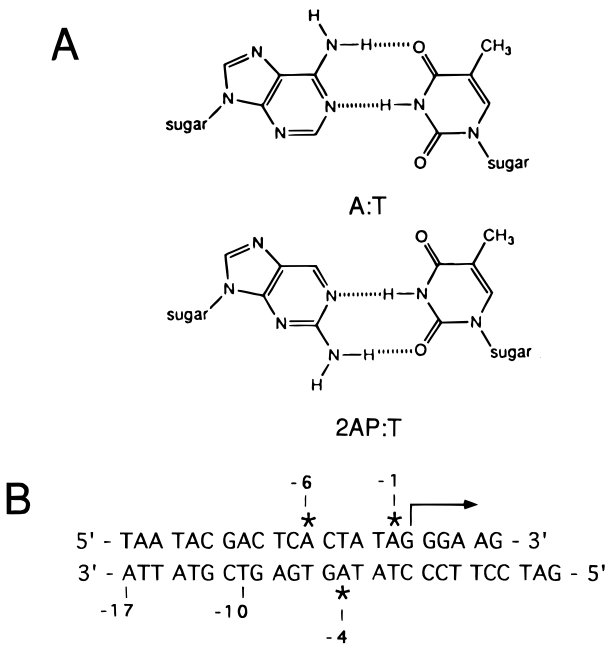

FIGURE 1: (A) Comparative illustrations of normal Watson−Crick base pairing between adenine and thymine (A:T) and base pairing between 2-aminopurine and thymine in a DNA duplex (2AP:T). (B) Sequence of the duplex DNA oligonucleotide used in this work. The DNA contains a T7 RNAP promoter −17 to +6. The promoter is different from the consensus class III promoter only at +5 and +6, and accommodates a *Bam*H1 site. The start site and the direction of transcription are shown with an arrow. 2-AP substitutions are indicated with a asterisk over the normal A residues.

(Raney et al., 1994). We exploited this property to monitor the kinetics of strand separation during open complex formation by T7 RNAP. We constructed a 23 bp template containing a slightly modified T7 promoter that had 2-AP substituted either at −1 (23-1) or at −6 (23-6) on the nontemplate strand or at −4 (27-4) on the template strand (Figure 1). Each template contained only a single 2-AP substitution, and was base-paired to its unmodified complementary strand, enabling us to monitor base unstacking and breaking of the H-bonds of that specific base pair. Base pair opening at these positions should translate into changes in fluorescence intensities, revealing whether promoter melting is concerted or progressive. These positions for 2-AP substitution were chosen based on the presumed initiation-melting domain reported by others (Chapman & Burgess, 1987; Chapman et al., 1988; Ikeda et al., 1992a,b; McAllister & Carter, 1980). Using a single-strand specific endonuclease, it was shown that the region between −6 and +2 (~8 nts) was nuclease-sensitive (Muller et al., 1989; Osterman & Coleman, 1981). Our footprinting data, using $KMnO_4$ as a probe for DNA unwinding, also indicated that this promoter region was melted in T7 RNAP−DNA complexes.[2]

Spectral Characteristics of 2-AP Oligonucleotides and T7 RNAP. Figure 2 shows the absorption and emission spectra of 23-1ss oligonucleotide and that of purified T7 RNAP. The 23-6 and 27-4 ss oligos showed similar absorption and emission spectra. The very large absoption maximum at 259 nm is typical of DNA base transitions excluding those of 2-AP. Unlike the unmodified oligomer, 23-1ss shows absorption bands (albeit very small) extending to at least

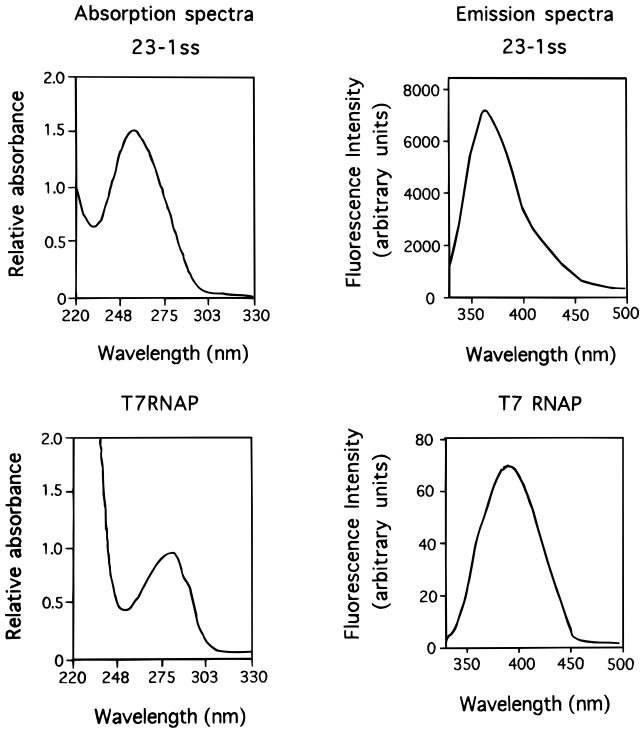

FIGURE 2: Uncorrected absorption and emission spectra of 23-1ss and T7 RNAP. The absorption spectra were recorded in a Beckman DU65 UV−VIS spectrophotometer. The excitation was at 310 nm. For emission scans, 23-1ss and T7 RNAP were at ~2 μM.

~320 nm. This absorption region (303−320 nm) indicates the presence of 2-AP [see also, for example, (Xu et al. (1994)]. T7 RNAP has an absorption maximum at 280 nm that is characteristic of the aromatic side chains. The strong absorption below 230 nm is due to the peptide $\pi \rightarrow \pi^*$ band. The emission maximum of 23-1ss is at 370 nm whereas for T7 RNAP it is at 390 nm. At 360 nm, where the emission was monitored in our experiments, the emission bands of 23-1ss were about a 150-fold greater than those of T7 RNAP, indicating that 2-AP fluorescence dominated that of T7 RNAP.

Temperature-Induced Separation of Promoter Strands. To illustrate that 2-AP fluorescence increases as the promoter DNAs go from a double-stranded to a partially single-stranded form, we carried out thermal melting. Figure 3 shows that all three templates behave almost identically when heated from room temperature (25 °C) to 70 °C and cooled slowly back to room temperature. The denaturation phase shows the expected sigmoidal shape that is indicative of a cooperative transition. The hysteresis of the renaturation phase may be perhaps because the DNAs were cooled more slowly than they were heated. The fluorescence intensity of different templates showed differences when melted (Figure 3; *y*-axis). This may be attributed to sequence-context differences in the positions of 2-AP in the templates [see, Bloom et al. (1993)]. These experiments confirmed that: (a) Indeed 2-AP fluorescence increased 2−3-fold when our templates go from double-stranded to a partially single-stranded form. As expected, upon cooling back to room temperature, the fluorescence intensity decreases to its original value because double-strandedness is restored. (b) A single 2-AP residue in our templates was a sufficiently dependable reporter of DNA melting. We also compared the steady-state emission spectra of 2-AP ss oligos with ds

[2] Sastry and Ross (1996), unpublished results.

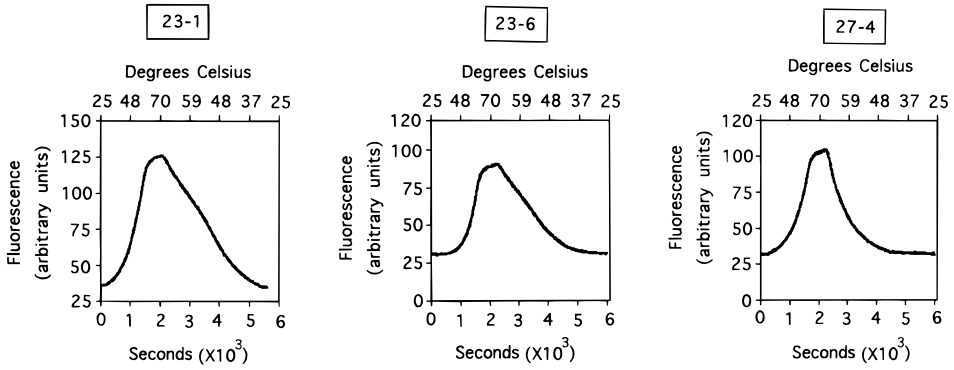

FIGURE 3: Melting behavior of ds templates as a function of temperature. Templates contained 2-AP substitutions at −1 (23-1) and −6 (23-6) on the nontemplate strand and at −4 (27-4) on the template strand. The concentration of DNA was ∼ 0.3 μM. The DNAs were gradually heated starting at 25 °C temperature (0 s) up to 70 °C and then cooled slowly. The temperature is indicated at the top of each graph in degrees centigrade. The temperature was directly read off the temperature-controlling water bath. The left-hand portion of each curve below 70 °C shows the heating phase while the right-hand portion shows the cooling phase. Note that the scale on the *y*-axis is different for 23-1 compared to 23-6 and 27-4 ds templates. The scale on the *x*-axis is given in (seconds × 10^3), i.e., kiloseconds. Each curve represents fluorescence intensity signal-averaged and digitized at 2 s intervals.

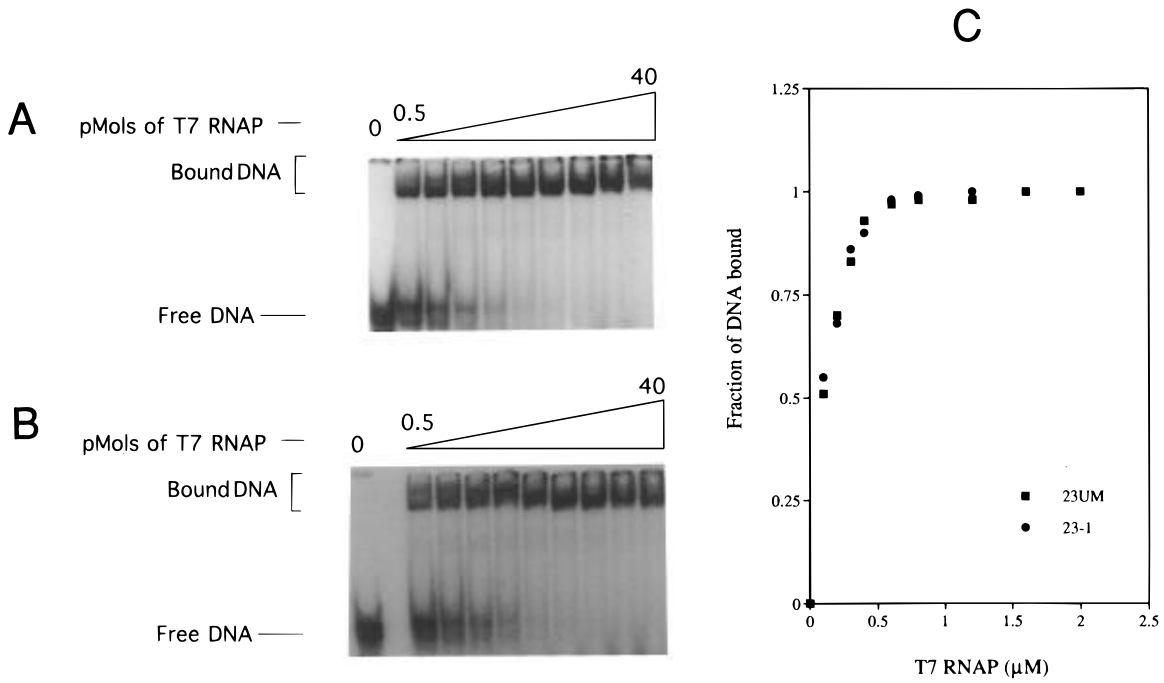

FIGURE 4: Gel-shift assay for DNA binding by T7 RNAP. (Panel A) Binding of T7 RNAP to 23UM template. (Panel B) Binding of T7 RNAP to 23-1 template. (C) Calculated binding isotherms. Squares represent 23UM, and circles represent 23-1. Each point in the graph represents an average of three independent determinations.

oligo. The fluorescence intensity was suppressed severalfold when the oligos were ds.

Binding of T7 RNAP Is Unaffected by 2-AP Substitutions. We tested whether our 2-AP-containing templates bind T7 RNAP with the same affinity as that of the wild-type template. Gel-shift assays indicated that T7 RNAP binds a 2-AP-substituted template (23-1) with the same stoichiometry as the unmodified template (Figure 4). A macroscopic binding constant was derived by fitting the data to a general power equation ($y = bx^m$). The slope ($m = dy/dx$) of the linear-transformed equation was equivalent to the binding constant. The derived macroscopic binding constant for 23UM and 23-1 was the same within experimental error ($K_b \sim 4 \times 10^7$ M^{-1}). Our results are in agreement with mutagenesis and footprinting studies showing that changes in residues −4 to +1 of the promoter did not affect the equilibrium binding constant of T7 RNAP to its promoter (Chapman et al. 1988). Competition experiments with low concentrations of nonspecific calf-thymus DNA (20 μg/mL) revealed that the specific gel-shifted bands due to T7 RNAP binding to promoter were not competed by nonspecific DNA. Since our oligo was only 23 bp and a typical footprint of T7 RNAP covers about 20 nts (Basu & Maitra, 1986; Ikeda & Richardson, 1986; Muller et al., 1989; Shi et al., 1988b), we infer that in our experiments only one molecule of T7 RNAP can be accommodated per DNA.

Poly(G)-ladder synthesis assays (see Figures 8 and 9) indicated that 2-AP-substituted templates supported transcription initiation by T7 RNAP in a manner similar to the unmodified template (data for other templates is not shown). These tests indicate that 2-AP substitutions in the promoter did not block binding or transcription initiation by T7 RNAP.

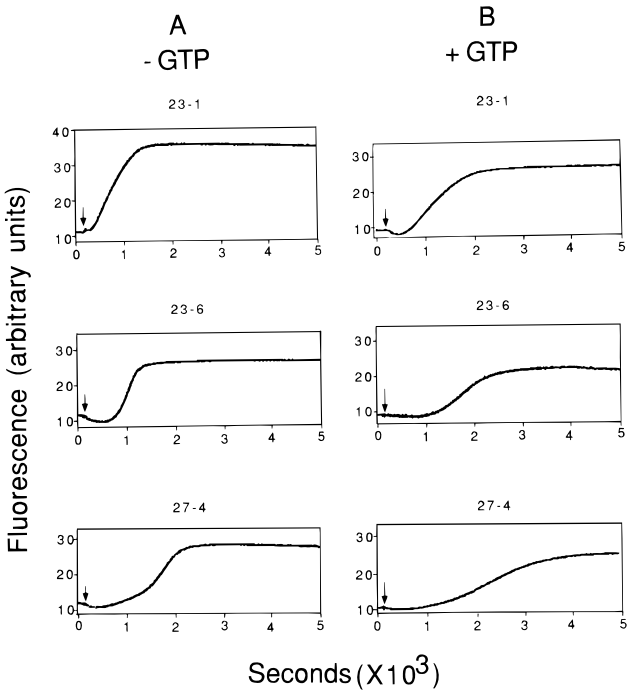

FIGURE 5: Opening of the promoter DNA by T7 RNAP in the presence and absence of GTP at 37 °C. Typical fluorescence curves are shown. These curves have been reproduced many times. T7 RNAP was present at a 1:1 molar ratio with DNA. The concentration of dsDNA was ~0.1 μM. Each curve represents fluorescence intensity signal-averaged and digitized at 2 s intervals. The templates are identified at the top of each curve. Note that the time coordinate is given in seconds $\times$ 10^3, i.e., kiloseconds.

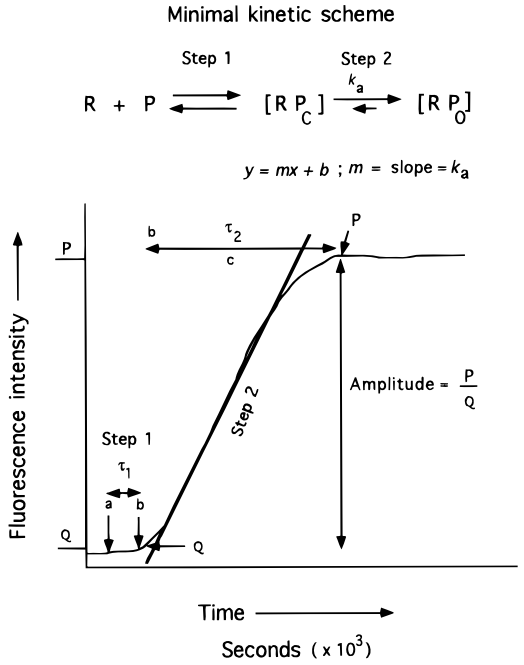

FIGURE 6: Diagrammatic representation of the data analysis procedure. At the top, a two-step minimal kinetic pathway for T7 RNAP open complex formation is shown. R is T7 RNAP, P is the promoter DNA oligo, RP_c is the closed complex, and RP_o is the open complex. An idealized steady-state fluorescence intensity curve is depicted. The *y*-axis is the fluorescence intensity increase, and the *x*-axis is time. Note that the time coordinate is given in seconds $\times$ 10^3, i.e., kiloseconds. See the text for the procedure used to obtain the various parameters in tables.

Opening of Promoter Strands by T7 RNAP. We conducted a series of pilot experiments to optimize the conditions for the following experiments. Various concentrations of 2-AP DNA and/or T7 RNAP were tested to attain an optimum fluorescence signal level. Titration of a fixed concentration of 2-AP DNA with different amounts of T7 RNAP showed that the kinetics of melting of promoter depended on the concentration of the enzyme (not shown), as reported for *E. coli* RNAP (Buckle et al., 1991). We concluded that a 1:1 enzyme to DNA molar ratio and a concentration of 0.1 μM were optimal.

Figure 5 shows a series of typical time-dependent steady-state fluorescence intensity changes observed by incubating each of the 2-AP templates with T7 RNAP in the absence or presence of the initiating nucleotide GTP. These changes have been consistently reproduced in several experiments. The arrows indicate the time of addition of T7 RNAP (~100 s in to the measurement). All the graphs show more or less the same generic shape. There is a lag time before the rise in fluorescence is detected following the addition of T7 RNAP (arrow). The fluorescence intensity (*y*-axis) increases with time (*x*-axis), indicating melting of the duplex DNA. At some point, the curves reach a plateau. Note that the time coordinate (*x*-axis) is shown in seconds multiplied by 1000, that is, in kiloseconds. Incubation of T7 RNAP with normal (no 2-AP) promoter DNA with identical sequence did not result in changes in fluorescence. After the fluorescence curve of a mixture of 2-AP promoter plus T7 RNAP reached a plateau, addition of 50 mM EDTA resulted in an immediate drop in fluorescence (not shown). Prolonging the incubation with EDTA decreased the fluorescence intensity to the base line indicating that chelation of Mg^{2+} resulted in polymerase dissociation and/or reversal of the complexes. This EDTA effect was not observed with either T7 RNAP alone or oligonucleotide alone. Because open complex formation is completely Mg^{2+}-dependent, the observed fluorescence intensity increase is indeed due to opening of the promoter by polymerase. Competition experiments with added excess nonspecific or promoter DNA were not appropriate in our assay because this increased the optical density of the samples, leading to inner-filter/light-scattering effects.

Deconvolution Procedure and Data Interpretation. We analyzed the steady-state fluorescence data on the basis of a widely-accepted minimal kinetic scheme for RNA polymerase action (Figure 6). This scheme has been previously applied to describe the pathway for "open complex" formation by *E. coli* RNAP [e.g., see Buckle et al. (1991) and deHaseth and Helmann (1995) and references cited therein], and is generally accepted for other procaryotic RNAPs. For the sake of simplicity, we have adopted the same scheme for T7 RNAP (see below for some caveats). In this scheme, we assume only two sequential steps for open complex formation. First, T7 RNAP (R) recognizes promoter DNA (P) to form closed complexes (RP_c; step 1). The closed complexes [RP_c] then isomerize at a certain overall rate, k_a, to open complexes [RP_o] (step 2). All fluorescence intensity curves (such as those in Figure 5) were deconvoluted based on this scheme. The generic shape of a fluorescence curve is shown in Figure 6. We extracted four parameters from each curve. (1) Step 1: We assumed that the encounter between RNAP and promoter is a second-order reaction involving a relatively fast and diffusion-controlled (~10^9 M^{-1} s^{-1}) phase that may be facilitated (von Hippel & Berg, 1989). The initial binding is followed by formation of competent

closed complexes [RP_c]. In some curves, a small decrease in fluorescence intensity is seen following the addition of T7 RNAP (arrow, Figure 5) before a monotonic rise is observed (e.g., 23-6 in Figure 5, panel A). Whereas in others the fluorescence intensity remains more or less constant during this period. We do not know the reason for this phenomenon, although it may suggest a DNA conformational change in the complex. In our simple kinetic analysis, we do not distinguish these events. Because the first phase of promoter-recognition by the enzyme at 37 °C is most probably extremely fast [in the tens to hundreds of millisecond time regime; e.g., Careri et al. (1975)] compared to the rate of fluorescence measurement by our spectrometer (set at 2 s), we assume that binding to promoter by T7 RNAP is "instantaneous". Hence, arrow "a" in Figure 6 indicates the start of the kinetic pathway. For our purpose here, the lag time (τ_1) is simply between time point "a" and time point "b", that is, the beginning and the end of step 1. Note that time point "b" is *before* the increase in fluorescence is first observed (arrow "Q", i.e., beginning of step 2 in Figure 6). Thus, τ_1 describes all events leading to closed complexation [RP_c] that include nonspecific promoter search, productive binding, conformational transitions, intermediates, and unstacking of bases, etc. τ_1 is an equilibrium time dimension for the association and dissociation rates. (2) Step 2 describes the isomerization of closed complexes [RP_c] to open complexes [RP_o]. The rate of fluorescence intensity increase is taken as a direct measure of the formation of [RP_o] because the reverse reaction [RP_o] to [RP_c], suggested by the short arrow in the kinetic scheme, is extremely slow compared to the forward rate. This assumption was shown to be correct for *E. coli* RNAP [e.g., see Buc and McClure (1985) and Buckle et al. (1991)]. The overall rate of open complex formation is obtained by fitting the linear portion of the fluorescence intensity buildup data to the equation of a straight line ($y = mx + b$; Figure 6). We assume that the rate k_a of isomerization of [RP_c] to [RP_o] is a first-order reaction and is given by the slope ($m = dy/dx$) of the linear equation (Figure 6). It is a cumulative macroscopic rate constant for open complex formation that includes all the intermediates. (3) Step 2: The lag time τ_2 (double arrow "c" in Figure 6). This is the time between the starting time point (Q) of step 2 (i.e., the first time point at which a rise in fluorescence intensity is observed) and the time point (P), following which a plateau is reached. τ_2 indicates the time taken for complexes to reach equilibrium between RP_c and RP_o. τ_2 is the average time for opening in a majority of the DNA molecules in the reaction mixture. This does not imply that there is complete unwinding in all the DNAs. (4) The ratio of P to Q gives the fold increase in fluorescence intensity, i.e., amplitude. The amplitude reports the average extent of opening in a majority of the DNA molecules in the reaction mixture.

Presently, no clear-cut models are available in the literature regarding the pathways for strand opening by T7 RNAP. Extrapolating the overall mechanism from *E. coli* RNAP to T7 RNAP may be the simplest approach, at least for now. There is a lack of concrete experimental data regarding T7 RNAP open complex formation. First of all, no forward or reverse rate constants for any steps in the minimal scheme in Figure 6 are known. RP_c has not been trapped. It is not clear if the equilibrium binding constant of T7 RNAP to a T7 promoter reflects RP_o or RP_c and/or a mixture of both states (Gunderson et al., 1987; Ikeda & Richardson, 1987). Moreover, there are some peculiarities of T7 RNAP initiation that have to be accounted for by any model for T7 RNAP strand opening and initiation. It has been reported that deletions of the nontemplate strand up to −6 did not affect k_m, or k_{cat}, two kinetic parameters that reflect binding and catalysis, respectively (Maslak & Martin, 1993).

Table 1: Kinetic Parameters for Open Complex Formation at 37 °C[a]

	k_a ($\times 10^7$ m^{-1} s^{-1})		lag time (min) (τ_1)		lag time (min) (τ_2)		amplitude	
template	−GTP	+GTP	−GTP	+GTP	−GTP	+GTP	−GTP	+GTP
23-1	2.8	1.5	2.1	5.5	21.7	34.2	3.0	2.5
23-6	3.1	1.1	7.9	12.5	15.6	35.8	2.7	2.2
27-4	0.6	0.1	6.6	13.3	32.2	68.3	2.6	2.4

[a] Average parameters ($n = 3$) were deconvoluted from curves such as those in Figure 5. The rationale is described in the text (see Results). k_a is the rate of open complex formation. τ_1 is the lag time (minutes) before strand opening. τ_2 is the lag time (minutes) before complete opening (plateau) in a majority of complexes after commencement of opening. Amplitude represents the extent of opening in a majority of DNA molecules.

Considering these facts, we decided not to pursue a more sophisticated treatment of our data in terms of solutions of model rate equations and computer-generated simulations, which would necessarily involve many more assumptions and extrapolations from other systems. We think this type of approach is premature for T7 RNAP and may be error-prone. Instead, we have used a minimalist approach that involved directly extracting the relevant parameters from our experimental data to make our conclusions. The same experimental conditions (T7 RNAP:DNA ratios, temperature, buffer, DNA sequence, etc.) were used for acquiring all the data. Therefore, any observed changes in fluorescence intensity are a reflection of the changes in the microenvironment at that specific 2-AP base pair.

Base Pairs Are Disrupted Asynchronously and Discontinuously. Table 1 summarizes the above parameters extracted from several graphs such as those in Figure 5.

Opening of base pairs −1 (23-1) and −6 (23-6) occurs at almost the same rate (k_a) whereas at position −4, base pair disruption is ∼5× slower (Table 1). Generally, disruption of base pairs at these positions is 2−3× or 5× slower in the presence of GTP as compared to its absence. Base pair disruption at −4 is 10× slower in the presence of GTP compared to at −1 or −6. Likewise, the lag times for binding, nonchemical conformational changes, etc. (τ_1), and for maximal opening (τ_2) at these base positions appear to be 2−3x longer in the presence of GTP than in its absence. This indicates that chemical transformation in the form of phosphodiester bond formation (because in the presence of GTP, T7 RNAP synthesizes a G-ladder; see Figure 8) is a rate-determining step for complete opening. In other words, base pair opening and RNA synthesis are linked. This linkage is probably not thermodynamic because if it were so, the breaking of the phosphoanhydride bond should provide extra energy [$\Delta G^\circ \sim -3.1$ kcal/mol nucleotide polymerized (Erie et al., 1992)], which might be expected to fuel the overall rate of melting. Therefore, we propose that catalytic steps (including GTP binding) and the physical steps such as conformational changes in both enzyme and DNA are kinetically rate-determining for base pair disruption

Table 2: Temperature-Induced Changes in Parameters for Strand Opening in the Absence of GTP[a]

template	temp (°C)	lag time (min) (τ_1)	lag time (min) (τ_2)	amplitude
23-1	23	12.5	77.3	2.2
	28	5.8	75.0	2.0
	37	3.3	20.8	2.1
	42	3.3	18.3	1.1
23-6	23	30.8	66.6	1.5
	28	18.3	50.8	2.1
	37	8.3	27.5	2.6
	42	8.3	29.2	1.1
27-4	23	ND	ND	ND
	28	ND	ND	ND
	37	4.5	33.8	2.2
	42	11.7	59.2	1.1

[a] Average parameters (n = 3) were deconvoluted from curves such as those in Figure 5. The rationale is described in the text (see Results). τ_1 is the lag time (minutes) before strand opening. τ_2 is the lag time (minutes) for complete opening in a majority of complexes (plateau) after commencement of opening. Amplitude represents the extent of opening in a majority of DNA molecules. ND indicates that parameters could not be determined for this template at these temperatures because there was no increase in fluorescence.

at these positions during T7 RNAP transcription initiation. This proposal assumes that the nonchemical (physical) steps are qualitatively the same in the presence or absence of GTP. It is generally assumed that the major rate-determining step is the slow step of isomerization of the closed complex (Buc & McClure, 1985; McClure, 1980, 1985). We add that the binding of the initiating nucleotide followed by chemistry is probably rate-determining as well for open complex formation. Based on τ_1 and k_a, it appears that −1 is disrupted first followed closely by −6 and then finally by −4. Because the amplitudes are almost the same for all three base pairs, we conclude that the average extent of opening by T7 RNAP at 37 °C is the maximum possible. Note that the 2-AP fluorescence increases about 2−3-fold upon complete denaturation of DNA [see Figure 3 and Bloom et al. (1993) and Raney et al. (1994)].

Thermodynamics of Base Pair Opening. Open complex formation is temperature-dependent (Buc & McClure, 1985; deHaseth & Helmann, 1995). We examined promoter opening as a function of temperature in our system. Fluorescence excitation and emission spectra are affected by temperature (Lakowicz, 1983). In the case of 2-AP, while the excitation maximum undergoes changes with temperature, the emission maximum changes very little (Xu et al., 1994). The fluorescence yields are greatly affected by temperatures close to the T_m of the duplex. However, in our case, (a) we are operating well below the T_m [calculated T_m of the 23-mer duplex was ∼85 °C using a published formula (Marmur & Doty, 1962)] and within a relatively narrow temperature range (23−42 °C), and (b) we are making conclusions from comparing the *relative* lag times and rates of fluorescence increase only *between* oligos under otherwise identical experimental conditions. Here, we are not concerned with spectral shifts or fluorescence quantum yields at these temperatures. Due to these considerations, our conclusions are not affected by solvent relaxation effects on fluorescence.

Table 2 lists the deconvoluted parameters from fluorescence curves at various temperatures. In general, lag times (τ_1) during which binding−conformational changes etc. in the enzyme and DNA occur (RP_c) before base pair disruption were longer at lower temperatures (<37 °C) than at higher temperatures (37 and 42 °C). Below 37 °C, we were unable to observe any changes in the fluorescence for 27-4 (ND in Table 2), indicating probably a much higher activation energy for disruption at −4 compared to at −1 or −6. τ_1 and τ_2 decrease with increasing temperature in the 23−37 °C range, consistent with decreasing activation energies at higher temperatures. Temperature effects on τ_1 for −1 and −6 are consistent with −1 being disrupted first followed by −6. Surprisingly, disruption of −4 bp appears to be slower at 42 °C compared to at 37 °C even though base pairs at −1 and at −6 showed almost the same behavior at both temperatures. It is possible that the microscopic protein−DNA contacts responsible for base pair disruption at −4 are somehow changed at 42 °C as compared to at 37 °C; 37 °C appears to be optimal for open complex formation as judged from all three parameters in Table 2. In general, the amplitude is lower at 42 °C. To verify that this was due to lower fluorescence yields at the higher temperature, we monitored the steady-state fluorescence intensity (excitation at 310 nm and emission at 360 nm) of ss and the corresponding ds oligos at 42 °C. The ratios of fluorescence intensity of ss over that of the ds oligos were as follows: 23-1 = 1.3; 23-6 = 1.3; 27-4 = 1.5. These ratios indicated that the lower amplitude at 42 °C was indeed due to lower fluorescence yields. This type of decrease in fluorescence intensity at higher temperatures has been shown by others also for some ss oligonucleotides containing 2-AP (Xu et al., 1994).

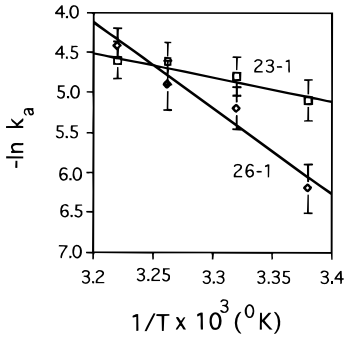

FIGURE 7: Arrhenius plot of the temperature dependence of the rate of isomerization (k_a). The E_a values for 23-1 and 23-6 were estimated to be 14 and 50 kcal mol^{-1}, respectively.

Figure 7 is an Arrhenius plot of the overall rate constant (k_a) for base pair opening. The derived activation energies (E_a) for 23-1 and 23-6 are 14 and 50 kcal mol^{-1}, respectively, in the 23−37 °C range. Because of the limited data set in this plot, there is a large error (25%) associated with these determinations. These activation energies are lower than those reported for the interaction of *E. coli* holo RNAP with λ_{pr} promoter (60−170 kcal mol^{-1}) (Roe et al., 1985) or *lac* UV5 promoter (120 kcal mol^{-1}) (Buc & McClure, 1985; Spassky et al., 1985). Assuming about 6−20 kcal mol^{-1} bp, our values indicate that for −1 we are probably reporting opening at that particular base pair. But for −6, E_a may include nearest-neighbor stacking interactions. Alternatively, it is possible that the sum total activation energies may reflect the sum total of nearest-neighbor unstacking/unwinding interactions for the region between −1 and −6 (6 bp; 64 /6 = 10.6 kcal mol^{-1} bp). If this is the case, the activation energies reported here are consistent with the proposal that

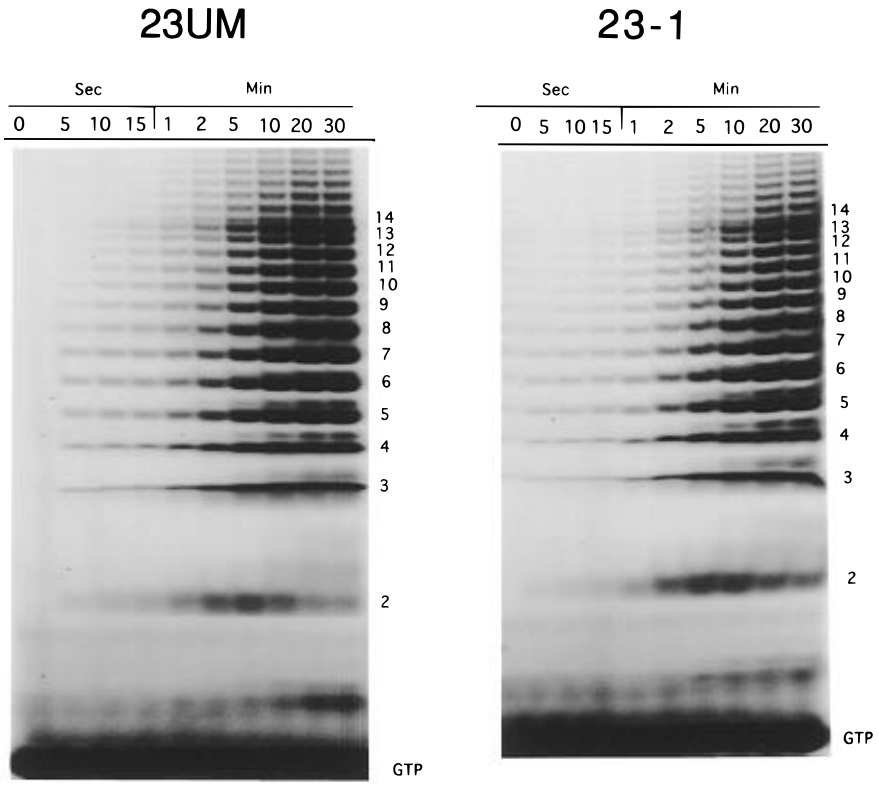

FIGURE 8: Kinetics of typical poly(G)-ladder synthesis. Autoradiographs of polyacrylamide (24%) gels show the poly(G)-ladders. Transcription was carried out in the presence of only GTP. Unincorporated radiolabeled GTP is at the bottom of the gel. The size of the ladder from 2 to 14 nts is shown on the right-hand side of each figure.

the total number of base pairs disrupted by T7 RNAP is smaller (6 or 7 bp) compared to that of *E. coli* RNAP (11−17 bp). No attempt was made to derive the E_a for 27-4 because we could not detect base pair opening for 27-4 (i.e., no increase in fluorescence) below 37 °C. Therefore, the data set was even more limited for this base pair.

Transcription Initiation. In an attempt to correlate the kinetics of strand opening with the rate of transcription initiation, we used a poly(G)-ladder synthesis assay. In the presence of GTP as the only nucleotide, T7 RNAP synthesizes a poly(G)-ladder that extends to ∼14 nts and abruptly tapers off (Gross et al., 1992; Martin et al., 1988; Sousa et al., 1992). The poly(G)-ladder is believed to be the result of reiterative slippage−synthesis at the three Cs, +1 to +3, on the template strand (Martin et al., 1988). Figure 8 shows an example of G-ladder synthesis on 23UM and 23-1 templates. It is seen that the G-ladder is qualitatively similar on both templates. A similar result was observed with 23-6 and 27-4 templates (not shown). Figure 9 shows quantitation of the rates of incorporation of GMP into G-ladders at various temperatures. The upper panels show the initial rates up to 1 min while the lower panels show the time course of transcription up to 30 min. All three templates show similar initial rates of activities. This is to be expected because the 2-AP mutations do not significantly change either promoter structure or activity. In agreement with τ_2 in Table 2 and Figure 7 the total incorporation rate (as indicated by the slopes of lines from 0−10 min) at 28 °C is ∼ 2−3 time slower than at higher temperatures. However, the magnitudes of lag times τ_1 and τ_2 in Table 2 do not directly reflect the transcription initiation rates in Figure 9. We did not observe any lag times before commencement of transcription (Figure 9A), in agreement with previous results (Ikeda et al., 1992a,b). Why? We think this can be explained in terms of the following scenario. Fluorescence experiments were done at an equimolar of DNA:T7 RNAP ratio. Depending on the stability of the initiation complexes, enzyme turnover could be minimal at high stability or extremely rapid if complexes are unstable. At most *E. coli* promoters, the reverse rate constant for $RP_o \rightarrow RP_c$ in (Figure 6) is very slow (3−10 times) compared to the forward rate constant $RP_c \rightarrow RP_o$ (deHaseth & Helmann, 1995; Gill et al., 1990; Goodrich & McClure, 1992; McClure, 1980, 1985; Schmitt & Reiss, 1995; Straney & Crothers, 1987). We may assume this to be true for T7 RNAP as well. Additionally, during slippage synthesis it is believed that ternary complexes are relatively stable (Borukhov et al., 1992; Macdonald et al., 1993; Muller et al., 1988; Sousa et al., 1992). These conditions allow the synthesis of G-ladder without enzyme dissociation, presumably keeping the strands open while abortion of transcript occurs. Thus, most of the DNA molecules are in a continually open state, at least within the time-scale of spectroscopic detection, hence the observed monotonic rise in fluorescence intensity.

A simpler explanation could be that ^{32}P transcript labeling during transcript initiation is a much more sensitive assay than fluorescence assay for detection of strand opening. Because enzyme turnover is probably faster than our rate of fluorescence recording, [^{32}P]GMP incorporation was easily detectable *before* fluorescence change could be detected. We think that one or more of the above explanations may account for the apparent lack of lag time in transcription initiation as opposed to fluorescence measurements.

DISCUSSION

A New Model for Base Pair Disruption during Open Complex Formation by T7 RNAP. Early transcription

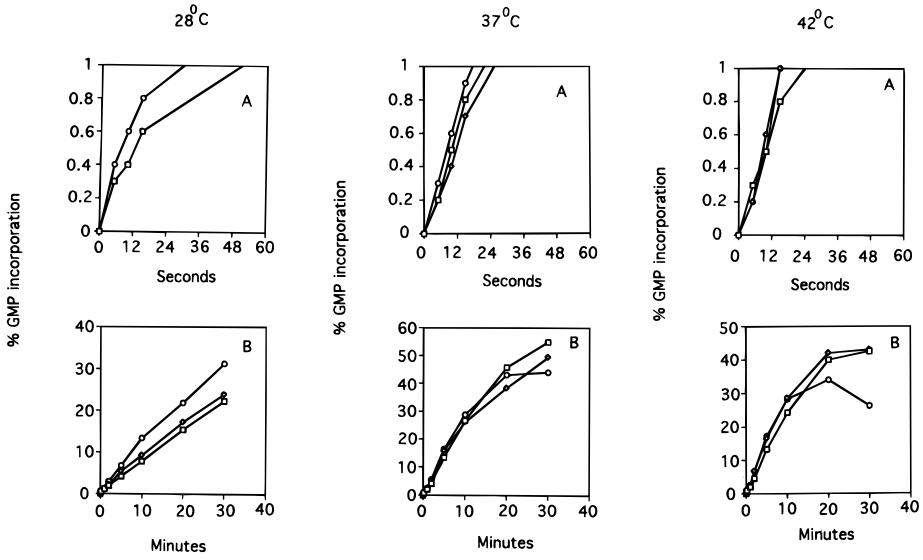

FIGURE 9: Rate of poly(G)-ladder synthesis on 2-AP templates at different temperatures. Upper panels (A) show initial rates (up to 60 s) of G-ladder synthesis, whereas the lower panels (B) show the full time course up to 30 min. Squares represent 23-1 template, diamonds represent 23-6 template, and circles represent 27-4. Note that in panel A at 28 °C the diamond symbols are masked by the square symbols because the points are identical. Each point is an average of three independent determinations. Each point was obtained from the integrated counts per minute representing all the bands in a G-ladder.

initiation experiments with *E. coli* RNAP led to the proposal that a binary complex undergoes transition from closed DNA to an open configuration (Mangel & Chamberlin, 1974). One key revision of the early model suggested that RNAP actively untwists the DNA, leading to base pair disruption and melting at upstream A·T-rich sequences in the promoter (Stefano & Gralla, 1982; Travers, 1987). A further refinement of the pathway for open complex formation proposed at least two schemes [see deHaseth and Helmann (1995)]. In one model, a base pair disruption event at or near the A·T sequences (−10), due to wrapping of the DNA around the polymerase, is followed by propagation of the bubble toward the +1 site. Others have envisioned melting as an all-or-none process involving a concerted breaking of the H-bonds holding the two strands together. These models have been applied to many procaryotic and eucaryotic RNAPs [e.g., see Ding and Winkler (1993), Juang and Helmann (1995), Kassavatis et al. (1992), and Meier et al. (1995)].

Early experiments with T7 promoters modified with base analogs suggested that certain changes in functional groups in the DNA grooves affected T7 RNAP transcription but others did not (Stahl & Chamberlin, 1978). Subsequently, several promoter point mutations were mapped that reduced polymerase binding but did not affect transcription (Chapman & Burgess, 1987; Chapman et al., 1988; Ikeda et al., 1992a,b). These results suggest that T7 RNAP transcription initiation is a highly complex process in which, at least in some instances, there is a lack of positive correlation between T7 RNAP transcription initiation on the one hand and binding on the other. The T7 RNAP promoter has been thought of as consisting of different functional domains for binding (−16 to −5) and melting−initiation (−4 to +5) (Chapman & Burgess, 1987; Diaz et al., 1993; McAllister & Carter, 1980). Owing to the low stability of promoter complexes and/or to their extremely transient nature, closed complexes have not been separately identified from open complexes. To date, direct experimental evidence for a melted region in open complexes is meager. Enzymatic and chemical probing has suggested that the region (or a subregion thereof) between −9 and +2 may be unwound (Muller et al., 1989; Osterman & Coleman, 1981).[2] Footprinting data showed that in the presence of GTP the contacts between T7 RNAP and promoter are more extensive than in its absence (Chapman et al., 1988; Ikeda & Richardson, 1986), suggesting that the conformations of polymerase/DNA complexes may be altered in the presence of GTP (Sen & Dasgupta, 1993). Here we have used a noninvasive and highly sensitive probe, viz., fluorescence, to understand the mechanism and kinetics of open complex formation in real-time. It should be noted that substitution of 2-AP for A switches the H-bond donor exocyclic amino group in the grooves (Figure 1A). When dA is substituted with 2-AP, the 6-amino nitrogen in the major groove of dA is now in the minor groove (Figure 1A). This is similar to the 2-amino group of G in a G·C base pair. In general, mutations from −17 to −5 positions affect binding but not initiation rates (Diaz et al., 1993). Substitution of G for A at −6 in the T7 RNAP promoter resulted in a small decrease in promoter-driven transcriptional activity (Ikeda et al., 1992c) but no difference in binding. Although the macroscopic binding constant is unaffected by 2-AP substitution (Figure 4), it is possible that some individual amino acid side chain contacts may have been altered in our modified promoter−T7 RNAP complexes. For example, the amino hydrogen may serve as a donor for some polar/charged side chains (Asp, Glu, Asn, Gln) (Rich, 1992; Saenger, 1984) of T7 RNAP. However, our conclusions are based on the assumption that the pathway for promoter melting is not altered by the 2-AP substitutions. We propose that −1 bp opens first followed by −6 bp, and these base pair disruption events then propagate in opposite directions to −4 (see Figure 1B). This is a new proposal and is different from the existing models of procaryotic open complex formation that are largely based on studies with *E. coli* RNAP (deHaseth & Helmann, 1995). Our thermodynamic and kinetic data (Tables 1 and 2; Figure 7) support this mechanism. Because we incorporated 2-AP only at −1, −4, and −6 positions, our experimental observation is limited to these base pairs.

Footprinting showed that the −1 sugar on the nontemplate strand is protected from OH radical attack, indicating a T7 RNAP contact at this base (Muller et al., 1989). The thymine methyl at −6 on the template strand is critical for promoter recognition (Maslak et al., 1993). While OH-radical footprinting data do not appear to show contact with −6A on the nontemplate strand (i.e., 23-6 2-AP in our case), this bp may still be disrupted because the T on the complementary strand is contacted. Footprinting also shows T7 RNAP contact with −4 on the template strand. In our scheme, polymerase makes contacts at or near −1 and −6 and induces a torsional stress (untwisting), perhaps by wrapping the DNA around itself. The −1 and −4 2-AP exocyclic amino nitrogens are in the same minor groove on one face of the helix whereas the −6 2-AP amino nitrogen is in the minor groove of the opposite face of the helix. We surmise that untwisting may occur via H-bonding of these functional groups. According to footprinting data, −1A and −4A are protected by the polymerase (Muller et al., 1989). So is −6T. Because polymerase makes contacts predominantly on one face of the helix (Muller, et al. 1989), in our model we imagine two sequential untwisting events at or near −1 followed quickly by another untwisting event at or near −6 followed by progressive melting toward −4. Since −4 bp is broken later than −1 and −6, this implies that DNA−protein contacts at −4 may be weaker or made later than at −1 and −6. The immediate prediction from this model is that there must be T7 RNA−promoter intermediate complexes between RP_c and RP_o signifying these base pair disruption events. Sensitivity to single strand-specific nuclease showed a major cleavage site at −6 and a minor one at −4, suggesting that these bp are disrupted in promoter complexes (Muller et al., 1989). Using $KMnO_4$ as a probe for unstacked/unwound bases, we found that −1T is particularly sensitive to this reagent.[2] These results support our model for bp disruption in the present work.

An unusual aspect of T7 RNAP transcription initiation is that a large portion (+4 to −5 or −6) of the nontemplate strand of the promoter can be deleted without affecting k_m and k_{cat}, two kinetic parameters that are indicative of binding and catalysis under certain conditions (Maslak & Martin, 1993). According to Martin, promoter melting is not a significant barrier for transcription initiation, and the promoter is designed for energetically facile strand opening. The activation energy for base pair disruption at −1 (Figure 7) and transcription initiation kinetics (Figure 9) appear to support this proposal.

ACKNOWLEDGMENT

We thank Dr. John Helmann for his critical comments on the manuscript, Dr. Eric Plum and Prof. Ken J. Breslauer for suggestions, and Prof. J. Lederberg for his general interest in the project.

REFERENCES

Amouyal, M., & Buc, H. (1987) *J. Mol. Biol. 195*, 795−808.

Basu, S., & Maitra, U. (1986) *J. Mol. Biol. 190*, 425−437.

Bloom, L. B., Otto, M. R., Beechem, J. M., & Goodman, M. F. (1993) *Biochemistry 32*, 11247−11258.

Borukhov, S., Sagitov, V., Josaitis, C. A., Gourse, R. L., & Goldfarb, A. (1992) *J. Biol. Chem. 268*, 23477−23482.

Buc, H., & McClure, W. R. (1985) *Biochemistry 24*, 2712−2723.

Buckle, M., Fritsch, A., Roux, P., Geiselman, J., & Buc, H. (1991) *Methods Enzymol. 208*, 236−259.

Careri, G., Fasella, P., & Gratton, E. (1975) *CRC Crit. Rev. Biochem. 3*, 141−164.

Chapman, K. A., & Burgess, R. R. (1987) *Nucleic Acids Res. 15*, 5413−5432.

Chapman, K. A., Gunderson, S. I., Anello, M., Wells, R. D., & Burgess, R. R. (1988) *Nucleic Acids Res. 16*, 4511−4524.

Cowing, D. W., Mecsas, J., Record, M. T., & Gross, C. A. (1989) *J. Mol. Biol. 210*, 521−530.

deHaseth, P. L., & Helmann, J. D. (1995) *Mol. Microbiol. 16*, 817−824.

Diaz, G. A., Raskin, C. A., & McAllister, W. T. (1993) *J. Mol. Biol. 229*, 805−811.

Ding, H. F., & Winkler, H. H. (1993) *J. Biol. Chem. 268*, 3897−3902.

Erie, D. A., Yager, T. D., & von Hippel, P. H. (1992) *Annu. Rev. Biophys. Biomol. Struct. 21*, 379−415.

Fox, J. J., Wempen, I., Hampton, A., & Doerr, I. L. (1958) *J. Am. Chem. Soc. 80*, 1669−1675.

Frey, M. W., Sowers, L. C., Millar, D. P., & Benkovic, S. J. (1995) *Biochemistry 34*, 9185−9192.

Gamper, H. B., & Hearst, J. E. (1982) *Cell 29*, 81−90.

Gill, S. C., Yager, T. D., & von Hippel, P. D. (1990) *Biophys. Chem. 37*, 239−250.

Goldberg, J., & Dunn, J. J. (1988) *J. Bacteriol. 170*, 1245−1253.

Goodrich, J. A., & McClure, W. R. (1992) *J. Mol. Biol. 224*, 15−29.

Gross, L., Chen, W. J., & McAllister, W. T. (1992) *J. Mol. Biol. 228*, 488−505.

Gunderson, S. I., Chapman, K. A., & Burgess, R. R. (1987) *Biochemistry 26*, 1539−1546.

Hochstrasser, R. A., Carver, T. E., Sowers, L. C., & Millar, D. P. (1994) *Biochemistry 33*, 11971−11979.

Ikeda, R., & Richardson, C. C. (1986) *Proc. Natl. Acad. Sci. U.S.A. 83*, 3614−3618.

Ikeda, R. A., & Richardson, C. C. (1987) *J. Biol. Chem. 262*, 3800−3808.

Ikeda, R., Lin, A. C., & Clarke, J. (1992a) *J. Biol. Chem. 267*, 2640−2649.

Ikeda, R., Ligman, C. M., & Warshamana, S. (1992b) *Nucleic Acids Res. 20*, 2517−2524.

Ikeda, R. A., Warshanna, G. S., & Chang, L. (1992c) *Biochemistry 31*, 9073−9080.

Juang, Y.-L., & Helmann, J. D. (1995) *Biochemistry 34*, 8465−8473.

Kassavatis, G. A., Blanco, J. A., Johnson, T. E., & Gieduschek, E. P. (1992) *J. Mol. Biol. 226*, 47−58.

Kovacic, R. T. (1987) *J. Biol. Chem. 262*, 13654−13661.

Krummel, B., & Chamberlin., M. J. (1989) *Biochemistry 28*, 7829−7842.

Lakowicz, J. R. (1983) *Principles of Fluorescence Spectroscopy*, Plenum Press, New York.

Macdonald, L. E., Zhou, Y., & McAllister, W. T. (1993) *J. Mol. Biol. 232*, 1030−1047.

Mangel, W. F., & Chamberlin, M. (1974) *J. Biol. Chem. 249*, 2995−3001.

Marmur, J., & Doty, P. (1962) *J. Mol. Biol. 5*, 109−118.

Martin, C. T., Muller, D. K., & Coleman, J. E. (1988) *Biochemistry 27*, 3966−3974.

Maslak, M., & Martin, C. (1993) *Biochemistry 32*, 4281−4285.

Maslak, M., Jaworski, M. D., & Martin, C. (1993) *Biochemistry 32*, 4270−4274.

McAllister, W. T., & Carter, A. D. (1980) *Nucleic Acids Res. 8*, 4821−4837.

McClure, W. R. (1980) *Proc. Natl. Acad. Sci. U.S.A. 77*, 5634−5638.

McClure, W. R. (1985) *Annu. Rev. Biochem. 54*, 171−204.

McLaughlin, L., Benseler, F., Graser, E., Piel, N., & Scholtissek, S. (1987) *Biochemistry 26*, 7238−7245.

Mecsas, J., Cowing, D. W., & Gross, C. A. (1991) *J. Mol. Biol. 220*, 585−597.

Meier, T., Scheckor, P., Wedel, A., Cellai, L., & Heumann, H. (1995) *Nucleic Acids Res. 23*, 988−994.

Muller, D. K., Martin, C. T., & Coleman, J. E. (1988) *Biochemistry 27*, 5763−5771.
Muller, D. K., Martin, C. T., & Coleman, J. E. (1989) *Biochemistry 28*, 3306−3313.
Nordlund, T. M., Anderson, S., Nilsson, L., Rigler, R., Graslund, A., & McLaughlin, L. W. (1989) *Biochemistry 28*, 9095−9103.
Nordlund, T. M., Xu, D., & Evans, K. O. (1993) *Biochemistry 32*, 12090−12095.
Osterman, H. L., & Coleman, J. E. (1981) *Biochemistry 20*, 4884−4892.
Raney, K. D., Sowers, L. C., Millar, D. P., & Benkovic, S. J. (1994) *Proc. Natl. Acad. Sci. U.S.A. 91*, 6644−6648.
Rich, A. (1992) *The Chemical Bond. Structure and Dynamics* (Zewail, A., Ed.) pp 31−86, Academic Press, New York.
Roe, J. H., Burgess, R. R., & Record, J. M. T. (1985) *J. Mol. Biol. 184*, 441−453.
Saenger, W. (1984) *Principles of Nucleic Acid Structure*, pp 385−431, Springer-Verlag, Berlin.
Schmitt, B., & Reiss, C. (1995) *Biochem. J. 306*, 123−128.
Sen, R., & Dasgupta, D. (1993) *Biochem. Biophys. Res. Commun. 195*, 616−622.
Sen, R., & Dasgupta, D. (1995) *Biophys. Chem. 57*, 269−278.
Shi, Y.-B., Gamper, H., & Hearst, J. E. (1988b) *J. Biol. Chem. 263*, 527−534.
Sousa, R., Patra, D., & Lafer, E. M. (1992) *J. Mol. Biol. 224*, 319−334.
Spassky, A., Kirkegaard, K., & Buc, H. (1985) *Biochemistry 24*, 2723−2731.
Stahl, S. J., & Chamberlin, M. J. (1978) *J. Biol. Chem. 253*, 4951−4959.
Stefano, J. E., & Gralla, J. D. (1982) *Proc. Natl. Acad. Sci. U.S.A. 79*, 1069−1072.
Straney, D. C., & Crothers, D. (1987) *J. Mol. Biol. 193*, 267−278.
Suh, W.-C., Ross, W., & Record, M. T., Jr. (1992a) *Science 259*, 358−361.
Suh, W.-C., Leirmo, S., & Record, M. T. (1992b) *Biochemistry 31*, 7815−7825.
Travers, A. A. (1987) *Crit. Rev. Biochem. 22*, 181−219.
von Hippel, P. H., & Berg, O. G. (1989) *J. Biol. Chem. 264*, 675−678.
Ward, D. C., Reich, E., & Stryer, L. (1969) *J. Biol. Chem. 244*, 1228−1237.
Xu, D., Evans, K. O., & Nordlund, T. M. (1994) *Biochemistry 33*, 9592−9599.
Zawadzki, V., & Gross, H. J. (1991) *Nucleic Acids Res. 19*, 1948.

BI960729D